Human Molecular Genetics, 1999, Vol. 8, No. 13 **2557–2566**

A novel RNA-binding nuclear protein that interacts with the fragile X mental retardation (FMR1) protein

Barbara Bardoni+, Annette Schenck and Jean Louis Mandel

Institut de Génétique et de Biologie Moléculaire et Cellulaire, CNRS/INSERM/ULP, BP 163, 67404 Illkirch Cedex, CU de Strasbourg, France

Received August 20, 1999; Revised and Accepted October 4, 1999

DDBJ/EMBL/GenBank accession nos AF159548 and AF159549

Silenced expression of the *FMR1* gene is responsible for the fragile X syndrome. The *FMR1* gene codes for an RNA binding protein (FMRP), which can shuttle between the nucleus and the cytoplasm and is found associated to polysomes in the cytoplasm. By two-hybrid assay in yeast, we identified a novel protein interacting with FMRP: nuclear FMRP interacting protein (NUFIP). *NUFIP* mRNA expression is strikingly similar to that of the *FMR1* gene in neurones of cortex, hippocampus and cerebellum. At the subcellular level, NUFIP colocalizes with nuclear isoforms of FMRP in a dot-like pattern. NUFIP presents a C2H2 zinc finger motif and a nuclear localization signal, but has no homology to known proteins and shows RNA binding activity *in vitro*. NUFIP does not interact with the FMRP homologues encoded by the *FXR1* and *FXR2* genes. Thus, these results indicate a specific nuclear role for FMRP.

INTRODUCTION

The fragile X mental retardation syndrome is a frequent cause of inherited mental retardation affecting ~1 in 4000 males and ~1 in 7000 females in Caucasian populations. In most affected males the syndrome is characterized by moderate to severe mental retardation, characteristic facial features and postpubertal macroorchidism. Behaviour in affected boys is often characterized by hyperactivity and some autistic features. Affected females have in general a milder mental handicap (1). The syndrome is associated with an unstable expansion of a CGG repeat located in the 5′-untranslated region (5′-UTR) of the fragile X mental retardation (*FMR1*) gene (2–4). The full mutation found in patients is characterized by an abnormal methylation pattern that shuts off transcription of the *FMR1* gene (5). *FMR1* codes for a series of protein isoforms derived from alternative splicing affecting the presence of exons 12 and 14 and the choice of acceptor sites in exons 15 and 17 (6,7). The largest of these proteins is 632 amino acids long. FMRP is widely, but not ubiquitously, expressed with abundant neuronal expression in brain, in particular in the hippocampus and the cerebellum (8–10). The full-length FMRP protein is localized in the cytoplasm (8), yet nuclear localization has occasionally been observed, and, in transfection studies, FMRP isoforms devoid of exon 14 sequences are localized in the nucleus (8,11).

FMRP contains regions similar to domains previously found in RNA-binding proteins (two KH domains and one RGG box); indeed, it is able to bind RNA homopolymers and some mRNAs (12–14). Recently FMRP was found associated to ribonucleoparticles (RNPs) in actively translating polyribosomes (15,16).

FMRP is endowed with a nuclear localization signal (NLS) (17,18) and a nuclear export signal (NES) (17–19), suggesting that it shuttles between nucleus and cytoplasm (20) and may be implicated in mRNA export from nucleus to cytoplasm. Alternatively a possible role in modulating the localization, stability and/or translation of its target mRNAs has also been hypothesized (for a review see ref. 21).

FMR1 is a member of a family of genes, whose other two known members (*FXR1* and *FXR2*) present high levels of similarity to *FMR1*. Like FMRP, FXR1P and FXR2P contain two KH domains and one RGG box; in addition, it has been demonstrated that FXR1P is associated with polysomes and binds RNA homopolymers *in vitro*. Comparison of the three proteins in man, mouse and *Xenopus* shows high level of similarity even in domains of unknown function. The three proteins are able to form homodimers and heterodimers (22–24). The three genes show an overlapping but clearly distinct pattern of expression in brain and testis (25). This suggests that these FMRP-related proteins, although structurally very similar, may have distinct functions during embryonic or adult life.

Apart from the KH domains, the NES and the RGG box, no specific function or features have been ascribed to other regions of FMRP that are well conserved in evolution. Such high level of conservation suggests that they may take part in protein–protein interactions. The NLS has been mapped already in the FMRP N-terminal region, but it has not been identified precisely and does not resemble classical NLSs.

A better knowledge of FMRP function is of major importance to understand the mechanism of fragile X syndrome. In order to find novel proteins interacting with FMRP that could play a role in the definition of FMRP function, we used the first 218 amino acids (N-terminal domain) of human FMRP as bait in a two-hybrid system in yeast (26). We have shown previously that a deletion construct corresponding to the first 114 amino acids of FMRP accumulates in the nucleus, suggesting that FMRP has a strong

+To whom correspondence should be addressed. Fax: +33 3 88 65 32 46; Tel: +33 3 88 65 34 14; Email: bardoni@igbmc.u-strasbg.fr

affinity for a nuclear component (18). The 218 amino acid N-terminal region has strong homology with *FXR1* and *FXR2* (23), is conserved during evolution (23) and contains the NLS activity (18). Here we report the identification of a novel protein interacting with FMRP. We have characterized the interaction between the two proteins both *in vitro* and *in vivo* by GST pull-down and co-immunoprecipitation. This FMRP-interacting protein, nuclear FMRP interacting protein (NUFIP), shows no homology to proteins of known function, and contains a C2H2 zinc finger motif and a putative NLS. NUFIP is localized in the nucleus in a dot-like pattern and appears colocalized with the nuclear isoforms of FMRP. *NUFIP* mRNA is widely expressed in adult tissues; however, results of *in situ* hybridization experiments in mouse brain show that *NUFIP* is expressed at high levels in neurons of cortex, hippocampus and Purkinje cells, like the *FMR1* gene. NUFIP shows RNA binding activity *in vitro*.

RESULTS

We have performed a yeast two-hybrid screening to identify putative interactors of the highly conserved N-terminal region of FMRP, which is devoid of identifiable functional motifs, although it contains the NLS activity (17,18).

A yeast expression vector encoding the N-terminal domain of the human FMRP fused to the DNA binding domain of the *Escherichia coli* transcription factor LexA (pBT-N-ter) was used as a bait. A mouse embryonic [embryonic day (E) 9.5–E12.5] library fused to the VP16 activation domain was used as prey (27). We performed the selection in the yeast strain L40 carrying both *HIS3* and *LacZ* reporters under the control of *LexA* responsive elements, in the presence of 25 mM 3-amino triazole. From ~4×10^6 clones screened, ~300 positive colonies corresponding to 10 different clones showed both histidine prototrophy and β-galactosidase activity, including the known interactors FXR1P (50 colonies) and FXR2P (1 colony). In order to test the capacity of our positive clones to interact also with the full-length protein we fused to VP16 a nuclear isoform of FMRP (ISO12) (11). β-galactosidase activity is moderately reduced when the bait is ISO12 (this is also true for the positive control *FXR2*) (Fig. 1A). However, we observed that ISO12 is less expressed than the N-terminus bait by western blot analysis on yeast protein extracts (data not shown). In addition, no β-galactosidase activity was observed in the yeast strain transformed only with the bait pBT-N-ter and the empty vector pASV3 (Fig. 1A).

Among the novel interacting clones we focused on the one that showed the highest β-galactosidase activity (Fig. 1A), in the same range as that elicited by the FXR2P control. It encodes a full-length protein of 484 amino acids in mouse, and is highly similar to human ESTs defining the orthologous human protein of 495 amino acids (72.8% identity and 81.1% similarity) (Fig. 1B). Two highly conserved domains are present in the middle of the protein (95% identity between man and mouse over 140 amino acids), and toward the C-terminus (100% identity over 42 amino acids). We propose to name these proteins h (human) and m (mouse) NUFIP. The amino acid sequences of the NUFIP proteins show no homology to proteins of known function. Using the PROSITE program several motifs were found from N- to C-terminus. A conserved proline stretch is present at position 39–44 (mNUFIP) and 44–49 (hNUFIP). This stretch is found in the context of a very proline-rich N-terminal domain. Twenty-seven proline residues are present in the first 105 amino acids of hNUFIP and in the corresponding first 98 amino acids of mNUFIP, 20 of them being at positions conserved between man and mouse. A C2H2 zinc-finger domain is present at position 165–192 (mNUFIP) and 174–201 (hNUFIP). A bipartite NLS is predicted at position 234–251 (mNUFIP) and 243–260 (hNUFIP). All these motifs are very highly conserved between man and mouse (Fig. 1B).

Characterization of the interaction between FMRP and NUFIP

The FMRP full-length protein (ISO1) was expressed as a fusion protein with glutathione *S*-transferase (GST) in a baculovirus system. The mNUFIP protein was produced and labelled with [^{35}S]methionine by *in vitro* transcription-translation using rabbit reticulocyte lysate. The GST–FMRP fusion protein immobilized on glutathione–Sepharose was incubated with either labelled mNUFIP or, as a positive control, the *in vitro* labelled FXR1P or FMRP. As a negative control we used luciferase. mNUFIP bound specifically to the immobilized GST–FMRP, as efficiently as the FMRP positive control (Fig. 2A). No binding to GST was observed. No signal was obtained for luciferase. Using increasing stringency conditions, we showed that mNUFIP, like FXR1P, interacts strongly with FMRP in the presence of 0.2 M NaCl, and interaction is still detectable at 0.5 M NaCl (Fig. 2B). The same results were obtained using hNUFIP (data not shown). In a reverse experiment, an NUFIP–GST column retained efficiently an *in vitro* translated FMRP isoform (ISO7) (Fig. 2C). Finally, we investigated whether the interaction could be indirect, mediated by RNA (as NUFIP itself has RNA-binding properties; see below). An experiment similar to the one reported in Figure 2A was performed after treatment of *in vitro* translated NUFIP and GST–FMRP beads with RNase A (100 μg/ml), RNase T_1 (40 U/ml) and DNase (100 μg/ml). This resulted only in a slight reduction of binding at 150 mM NaCl (also observed for an FXR1P positive control) (data not shown), indicating that a direct protein–protein interaction is indeed present.

We confirmed the interaction by co-immunoprecipitation in COS cells cotransfected with a vector expressing the *hNUFIP* full-length cDNA or its deletion constructs (Fig. 3A) and with a vector expressing ISO12, a nuclear isoform of FMRP (11). For this experiment we raised an anti-NUFIP antibody against a synthetic polypeptide corresponding to the C-terminus of the human NUFIP protein (amino acids 421–442). One rabbit antiserum was obtained and, after purification on an affinity column, its specificity was determined by both immunoblotting and immunofluorescence staining using HeLa and COS cells transfected with an expression vector for *hNUFIP*.

Cell extracts from cotransfected COS cells were immunoprecipitated using the polyclonal anti-NUFIP antibody (no. 1375), followed by immunoblotting with the monoclonal anti-FMRP antibody 1C3 (8). The control was performed by co-immunoprecipitation of the same cell extracts using a polyclonal anti-huntingtin antibody (no. 566) (28). ISO12 was co-immunoprecipitated by the anti-NUFIP antibody, but not

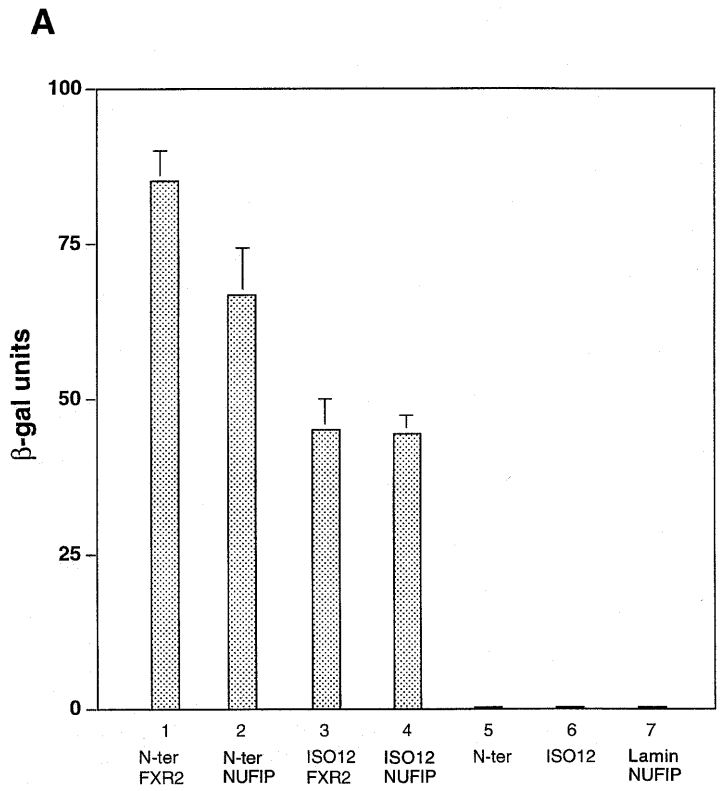

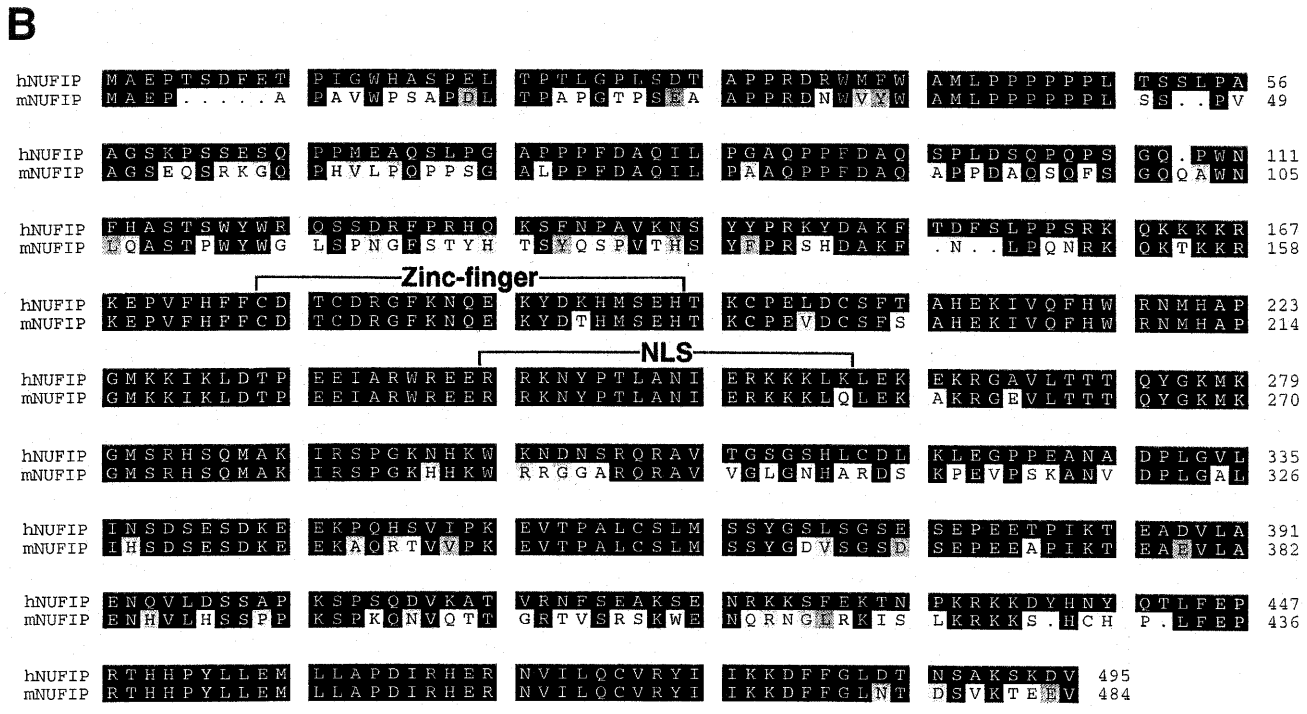

Figure 1. (**A**) β-galactosidase activity test for interaction in the two-hybrid system. Baits were the N-terminal region of FMRP and ISO12 (nuclear isoform of FMRP) and preys were mouse FXR2P (bars 1 and 3) (derived from clone N21 in our two-hybrid screening) and NUFIP (bars 2 and 4) (corresponding to clone N43 in our two-hybrid screening). The negative controls (bars 5–7) were, respectively, the two baits alone and the prey with lamin fused to the DNA binding domain of LexA. (**B**) Alignment of human and mouse NUFIP amino acid sequences. The putative C2H2 zinc finger and NLS are indicated. The cDNAs were established as described in Materials and Methods.

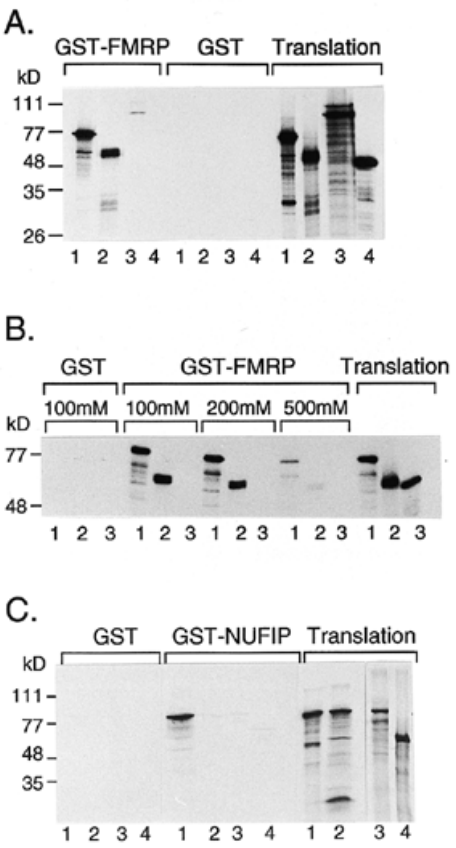

Figure 2. Interaction *in vitro* between FMRP full-length protein and NUFIP. (**A**) GST pull-down assay using 1 µg of the fusion protein GST–FMRP produced in a baculovirus system and the following *in vitro* translated proteins: lanes 1, FMRP ISO7 (positive control); lanes 2, mNUFIP; lanes 3, N44, a clone obtained in two-hybrid screening; lanes 4, luciferase (negative control). The binding was carried out in presence of 100 mM NaCl. (**B**) The GST pull-down experiments were performed in increasingly stringent conditions (from 100 to 500 mM NaCl). Lanes 1, $FXR1P_{78}$ (30); lanes 2, mNUFIP; lanes 3, luciferase. NUFIP is still detectable at 500 mM NaCl. The negative control with GST was done only in the least stringent condition. (**C**) GST pull-down assay using 1 µg of the fusion protein GST–hNUFIP produced in bacteria and the following *in vitro* translated proteins: lanes 1, FMRP ISO7 (positive control); lanes 2, $FXR1P_{78}$; lanes 3, FXR2P; lanes 4, luciferase (negative control). The binding was carried out in the presence of 100 mM NaCl. In each gel, 10% of each translation product or 20% of the eluate from glutathione beads was loaded. The absence of binding to GST alone demonstrates the specificity of the interaction.

by the unrelated antibody, in cell extracts obtained from COS cotransfected with full-length or different C-terminal deletion constructs of NUFIP (Fig. 3B and C). These experiments substantiated the *in vivo* interaction between NUFIP and FMRP and indicate the presence of an interaction region in the C-terminal half of NUFIP (Fig. 3C). In the same set of experiments, an N-terminal huntingtin construct could not be co-immunoprecipitated with ISO12 (data not shown). In other GST pull-down experiments, we found that both a C-terminal construct (254–495 amino acids) and an N-terminal construct (1–254 amino acids) are able to interact efficiently at 250 mM NaCl with GST–FMRP (data not shown), suggesting that two FMRP-interacting domains in NUFIP could exist.

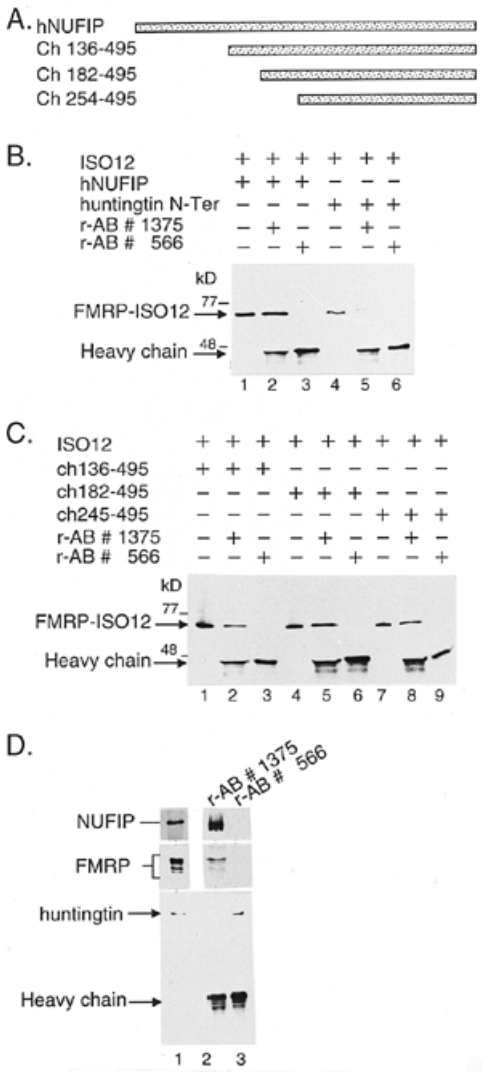

Figure 3. (**A**) Scheme of deletion constructs derived from hNUFIP and used for immunoprecipitation studies. (**B**) *In vivo* interaction between NUFIP and FMRP tested by co-immunoprecipitation. Cell extract of COS cells cotransfected with ISO12 and hNUFIP or an unrelated huntingtin construct was immunoprecipitated using an anti-NUFIP antibody (no. 1375) or an anti-huntingtin antibody (no. 566). Lanes 1 and 4, 2.5% of total cell extract was loaded; lanes 2, 3, 5 and 6, 15% of co-immunoprecipitated product was loaded. Monoclonal antibody 1C3 was used to reveal ISO12. (**C**) *In vivo* interaction between FMRP and NUFIP deletion constructs. Co-immunoprecipitation was carried out as above using extracts of COS cells cotransfected with ISO12 and different N-terminally deleted hNUFIP constructs [corresponding to mouse constructs 2–4 in (A)] or an unrelated huntingtin construct. Lanes 1, 4 and 7, 2.5% of the total extracts was loaded; lanes 2, 3, 5, 6, 8 and 9, 15% of immunoprecipitated products was loaded. ISO12 was revealed by monoclonal antibody 1C3. (**D**) *In vivo* interaction between endogenous NUFIP and FMRP. Co-immunoprecipitation was carried out as described above using HeLa cell extracts. Lane 1, 1% of the total extract was loaded; lane 2, 10% of co-immunoprecipitated product with antibody no. 1375 was loaded; lane 3, 10% of the co-immunoprecipitated product with antibody no. 566 was loaded. Each lane was revealed with antibodies nos 1375, 1C3 and 566, respectively.

To further test the ability of NUFIP to interact *in vivo* with FMRP, we co-immunoprecipitated the endogenous proteins. HeLa cell extract was immunoprecipitated with the polyclonal antibody no. 1375 (anti-NUFIP) and with the antibody no. 566

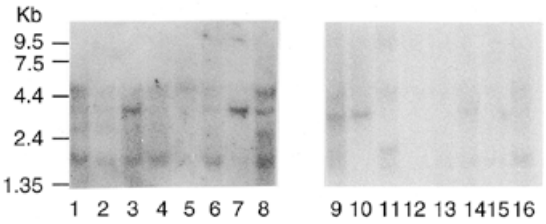

Figure 4. Northern blot analysis of *NUFIP* expression in human tissues; *hNUFIP* cDNA was used as a probe on a blot containing poly(A)+ RNA from different tissues (Clontech). Lane 1, spleen; lane 2, thymus; lane 3, prostate; lane 4, testis; lane 5, ovary; lane 6, small intestine; lane 7, colon (mucosal lining); lane 8, peripheral blood leukocyte; lane 9, heart; lane 10, brain; lane 11, placenta; lane 12, lung; lane 13, liver; lane 14, skeletal muscle; lane 15, kidney; lane 16, pancreas. After hybridization in ExpressHyb Hybridization Solution (Clontech), the blots were washed twice in 0.2% SSC, 0.1% SDS at 65°C.

(anti-huntingtin) (28), followed by immunoblotting with the same antibodies and the polyclonal 1C3 (anti-FMRP) (8) (Fig. 3D). FMRP isoforms were co-immunoprecipitated by the no. 1375 antibody but not by the no. 566 antibody (Fig. 3D).

Interaction with FXR1P and FXR2P

As FXR1P and FXR2P show 69.5 and 68.9% identity, respectively, to the 218 amino acid FMRP N-terminal region (22,23) used as bait, we decided to test interaction between mNUFIP and human FXR1P/FXR2P. We cloned in the pBTM116m vector the *FXR1* or *FXR2* regions corresponding to the FMR1P N-terminus. We cotransformed the L40 yeast strain with *FXR1* or *FXR2* deletion constructs and the *mNUFIP* (clone N43). Interaction between mNUFIP and FXR1P or FXR2P was tested by evaluation of the β-galactosidase activity in cotransformed yeast colonies. No β-galactosidase activity was observed in all analysed colonies. In this experiment, we used as a positive control the mouse clones corresponding to FXR1P and FXR2P (N27 and N21, respectively) that we found in two-hybrid screening. As expected, each construct was able to homo- and heterodimerize. We also tested the expression level of FXR2P and FXR1P by immunoblotting of yeast protein extract (using an anti-lexA antibody): an expression level comparable with the bait (pBT-N-ter) expression level was observed. To confirm these results, we performed some GST pull-down experiments using hNUFIP fused to GST (produced in bacteria) and *in vitro* translated human FXR1P and FXR2P. We did not observe interaction between hNUFIP and FXR1P or FXR2P in presence of 100 mM NaCl (Fig. 2C).

Expression of the *NUFIP* gene

Northern blot hybridization using *mNUFIP* cDNA as a probe detected in total RNA from mouse cerebellum a transcript of ~1.8 kb (data not shown), a length similar to the 1657 bp cDNA sequence derived from the analysis of 7 cDNA clones (see Materials and Methods).

A human cDNA sequence of 3462 bp [ending with a poly(A) tail] was derived from two overlapping ESTs. Northern blot hybridization using *hNUFIP* cDNA as a probe detected a signal in poly(A)+ RNAs from 16 different human tissues (Fig. 4). Bands of ~1.8, ~3.5 and ~5 kb were observed in various tissues suggesting the presence of alternatively spliced or polyadenylated mRNA species. Indeed four human EST

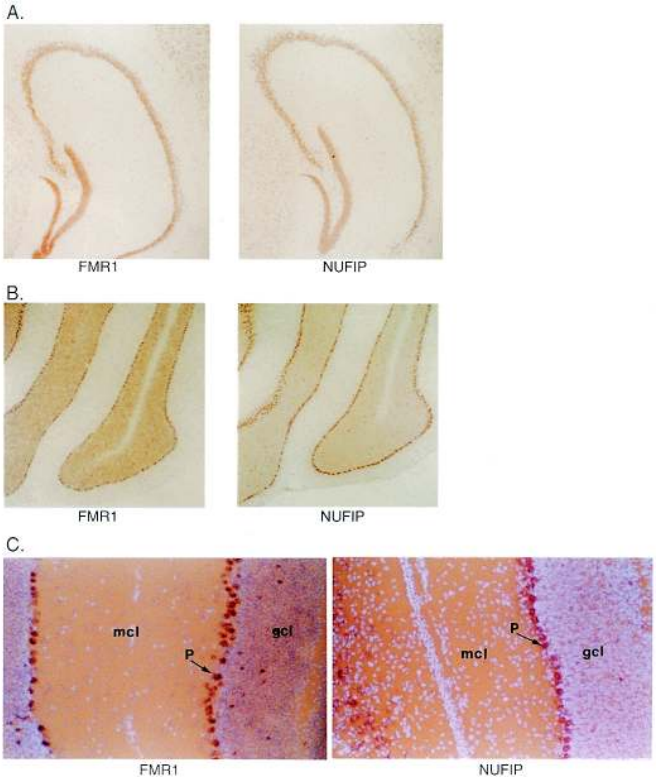

Figure 5. *In situ* hybridization using digoxigenin-labelled *FMR1* and *NUFIP* probes. (**A**) Expression in hippocampus. Part of the cortex labelling is visible in the right corner. (**B**) Expression in cerebellum. (**C**) Magnification of cerebellum: P, Purkinje cell; mcl, molecular cell layer; gcl, granular cell layer.

sequences occur 18 bp after an AATAAA polyadenylation signal present at position 1655 (the first nucleotide of the initiation codon is taken as position 1) and thus corresponding to the ~1.8 kb band. For brain RNA a single band was observed at ~3.5 kb corresponding to the length of the sequenced cDNA (from a neuronal cell line library) (Fig. 4).

We also compared the distribution of the *FMR1* and the *mNUFIP* transcript by *in situ* hybridization on mouse brain sections using RNA probes labelled with digoxigenin. For both probes, strong labelling of neurons was observed in hippocampus and in cortex (Fig. 5A). In the cerebellum, the two genes were highly expressed in Purkinje cells, whereas, in the granular cell layer, *FMR1* expression appears comparatively higher than that of *NUFIP* (Fig. 5B and C). Expression of both genes in the molecular layer appeared very low. These findings indicate that *NUFIP* is expressed in neurons and not in glial cells in the brain, similarly to *FMR1*.

Subcellular localization of NUFIP

An expression vector encoding the *mNUFIP* clone fused to green fluorescent protein (GFP) was used in transfection experiments in HeLa cells. The fusion protein was localized in the nucleus in a dot-like distribution (Fig. 6E), and colocalized with cotransfected FMRP nuclear isoform ISO12 (Fig. 6A–C). The same results were obtained transfecting cells with hNUFIP cloned in a eucaryotic expression vector and revealed using the polyclonal no. 1375 antibody (Fig. 6J) and in cotransfected

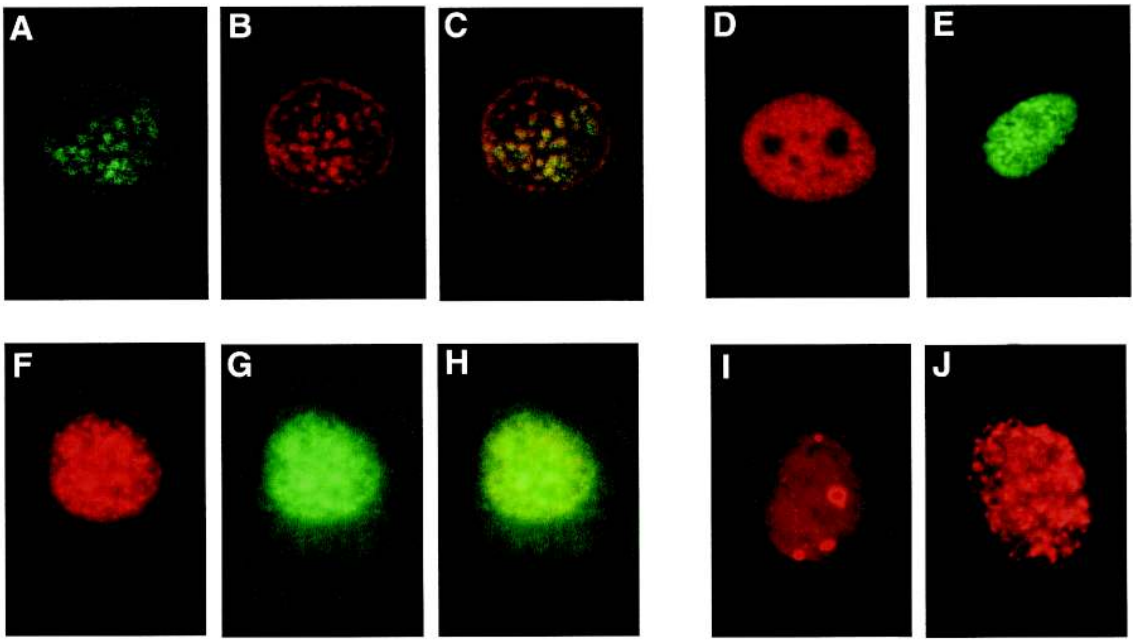

Figure 6. Confocal (A–E) and light (F–J) microscopy analysis of HeLa cells transiently transfected with ISO12 (FMRP nuclear isoform), mNUFIP fused to GFP (GFP–mNUFIP) and hNUFIP cloned in pTL1. ISO12 was revealed by monoclonal antibody 1C3 (B, D, G and I), whereas hNUFIP was revealed by polyclonal antibody no. 1375 (F–J). (**A**) Nuclear pattern of GFP–mNUFIP in cell cotransfected with ISO12. (**B**) Nuclear pattern of FMRP ISO12 in cell cotransfected with GFP–mNUFIP. The combined images are shown in (**C**). HeLa cells transfected with the ISO12 alone (**D**) and with GFP–mNUFIP alone (**E**). (**F**) Nuclear pattern of hNUFIP in cell cotransfected with ISO12. (**G**) Nuclear pattern of FMRP ISO12 in cell cotransfected with hNUFIP. The combined images are shown in (**H**). HeLa cells transfected with the ISO12 alone (**I**) and with hNUFIP alone (**J**).

cells with ISO12 (Fig. 6F–H). In cells transfected only with FMRP ISO12 a more homogeneous nuclear staining of ISO12 was observed by conventional immunofluorescence on confocal microscopy (Fig. 6D) or on light microscopy (Fig. 6I). These results suggest that nuclear localization of FMRP may be modulated by interaction with NUFIP.

RNA-binding activity of NUFIP

The zinc-finger motif is known to be an RNA-binding module in some cases. To investigate the capacity of NUFIP to bind to RNA homopolymers *in vitro*, we synthesized mNUFIP in a wheat germ system (lacking endogenous FMRP). Full-length mNUFIP protein binds poly(G) and, less efficiently, poly(U), but not poly(A) or poly(C) (Fig. 7A). This result was confirmed in an RNA homopolymer-binding assay using his-tag-hNUFIP expressed in bacteria, revealed by the anti-NUFIP antibody. The binding to poly(G) was more efficient than binding to poly(U) (data not shown). This pattern of binding appears similar to that observed previously for FMRP (12,13,29).

hNUFIP fused to GST and produced in bacteria was also used to carry out a north-western experiment. The recombinant protein interacts with RNA in this assay as well as FMRP, while no binding was observed for GST (Fig. 7B) and an unrelated protein, ovalbumin (data not shown).

DISCUSSION

FMRP is an RNA-binding protein having both an NLS and an NES, which led to the suggestion that it shuttles between the nucleus and cytoplasm (17–19). However, all the isoforms detectable at the protein level *in vivo* appear cytoplasmic (8,11). In the cytoplasm, FMRP is associated to actively translating polysomes via RNA, being part of an RNP complex (15,16). FMRP is thought to be implicated in mRNA export from nucleus to cytoplasm (for a review see ref. 21). However, the precise physiological role of FMRP is unknown, and it is also unknown whether FMRP is involved in RNA metabolism in the nucleus. The 'nuclear' isoforms lacking the NES whose existence was predicted by RT–PCR, have not been unequivocally detected *in vivo* (11) and are likely to be present only at low level.

Only two proteins interacting with FMRP have been identified previously: FXR1P and FXR2P, showing high similarity to FMRP and probably endowed with a related but distinct function (22,23,25,30).

Our previous results suggested that the FMRP N-terminal region, which contains the NLS activity and the homo- or heterodimerization domain but lacks known functional motifs, has an affinity for the nucleus (18). Using the yeast two-hybrid assay to identify novel proteins that interact with the N-terminal domain of FMRP, we identified 10 positive clones, including the known interactors FXR1P and FXR2P. The best interactor was a novel nuclear protein, NUFIP, which presents no homology with known proteins. It contains a bipartite NLS and a C2H2 zinc-finger motif. NUFIP is localized in the nucleus in a dot-like pattern and colocalizes with FMRP nuclear isoforms in transfection assays. In transfection experiments, nuclear FMRP isoforms, such as ISO12 (11), show a homogeneous distribution in the nucleus, excluding the

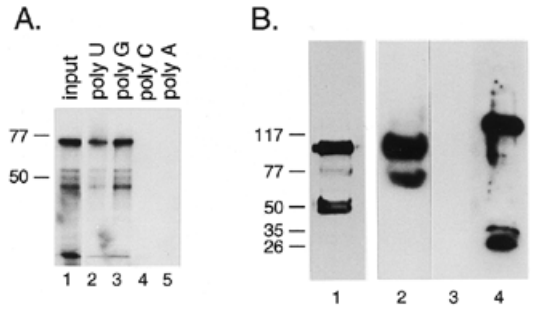

Figure 7. RNA-binding activity of m- and hNUFIP. (**A**) Binding to the RNA homopolymer beads. mNUFIP binds preferentially to poly(G) and, less intensely, to poly(U) in the presence of 0.25 M NaCl. (**B**) North-western analysis performed using recombinant GST–hNUFIP protein (lane 2), GST alone (lane 3), GST–FMRP (lane 4) and, as probe, RNA transcribed from the polylinker of pBluescript. Lane 1, recombinant GST–hNUFIP was analysed by immunoblotting with antibody no. 1375, as a control. Two bands of degradation are present. Lane 2, the full-length (~100 kDa) protein fused to GST and the larger degradation product bind to RNA.

nucleolus. When cotransfected with *NUFIP*, FMRP ISO12 shows a dot-like distribution, perfectly overlapping with that of its nuclear partner, indicating that co-expression in the nucleus modifies, in this experimental system, the distribution of FMRP ISO12. This suggests that interaction of NUFIP and FMRP in the nucleus may target the latter to specific subdomains relevant for its putative nuclear function.

The interaction between the two proteins was confirmed *in vitro* by GST pull-down experiments and *in vivo* by co-immunoprecipitation in mammalian cells and it is still present under high salt conditions. Our failure to detect interaction between FXR1P or FXR2P and NUFIP is surprising, given the high degree of similarity of FXR1P and FXR2P to FMRP. It will thus be interesting to map more precisely the site of interaction in the N-terminal domain of FMRP. Recent results from Tamanini *et al*. (20) suggest that FXR2P localizes to the nucleolus when nuclear export is inhibited. It is therefore possible that the three homologous proteins interact with different proteins/sites within the nucleus and may thus have specialised rather than overlapping functions.

In mouse adult brain, *FMR1* and *NUFIP* genes show a very similar neuronal expression pattern, with high expression in regions involved in cognitive function (cortex and hippocampus). This suggests that the interaction between FMRP and NUFIP is relevant for neuronal function in *vivo*.

We have also shown that NUFIP can bind RNA *in vitro*, and it could thus be involved in RNA metabolism in the nucleus. Mutation of the mNUFIP zinc finger does not prevent the binding of the *in vitro* translated product to poly(G) and poly(U) (our unpublished data), suggesting that a novel RNA binding motif may be present in this protein.

A current accepted model suggests that FMRP binds some specific mRNAs in the nucleus and then moves to the cytoplasm as a part of an RNP complex, where it is involved in delivery of mRNA to ribosomes (21). It will be important to determine whether NUFIP is part of such a nuclear RNP complex together with FMRP and/or whether the NUFIP/FMRP complex may play a specific role in post-transcriptional modification in the nucleus. Recently PML bodies were found to be the nuclear regions in which nascent RNA is present (31). Thus, it could be interesting to study whether nascent RNA is present in the nuclear dots in which NUFIP is localized. The identification of the nuclear domain where NUFIP is localized and the definition of the specific RNA sequences bound by FMRP/NUFIP complex will be an important step in the understanding the function of both proteins.

The specificity of interaction with FMRP, exemplified by the apparent absence of interaction with FXR1P and FXR2P, suggests that the lack of this interaction may play a role in the fragile X syndrome phenotype. Furthermore, the *NUFIP* gene may be a candidate for cases of mental retardation. It will be interesting to study the expression of the *NUFIP* gene during development in order to correlate its expression to *FMR1* expression and to the physical features in the fragile X syndrome. Understanding the function of NUFIP is an essential step in the definition of the molecular and developmental mechanisms by which the absence of *FMR1* expression produces the fragile X syndrome.

MATERIALS AND METHODS

Two-hybrid screening in yeast

An ISO7 construct (11) was digested with *Eco*RI and *Xho*I, generating a fragment of 654 bp that was cloned in the vector pBTM116m (27). This construct was named pBT-N-ter.

The yeast strain L40 [his 3D200 trp1-901 leu2-3, 112 ade2 LYS::(lexAop)4–HIS3 URA3::(lexAop)8–lacZ gal4 gal80] was used for transformations and assays. Yeast transformation and growth were performed as described (27,32). An E9.5–12.5 mouse embryo cDNA library in the vector pASV3 (33) was transformed into the yeast strain L40 already harbouring pBT-N-ter. The transformants were plated onto appropriate selective medium (SC) supplemented with 25 mM 3-amino-triazole (Sigma, St Quentin Fallavier, France). The cDNAs of positive plasmids were isolated by growing the His^+/β-$galactosidase^+$ colonies in SC media overnight, lysing the cells with acid-washed beads, electroporating the bacterial strain HB101 (leuB auxotrophic) with the yeast lysate and plating onto M9 (–Leu) plates (27). Liquid β-galactosidase assays were performed with 10 independent measurements as described (34).

Expression of recombinant FMRP

The plasmid ISO1 (11) was amplified using the primers GGGGCTAGCATGGAGGAGCTGGTGGTGGAAG and GGGGCTAGCTTAGGGTACTCCATTCACGAG, both containing an *Nhe*I site. The obtained fragment was digested with *Nhe*I and cloned in the PVL1393-GST-HMK-His5 vector (35). The PCR reaction consisted of 1 cycle at 94°C (2 min), 30 cycles of 94°C (10 s), 57°C (10 s) and 72°C (20 s) and 1 cycle at 72°C (5 min), and was performed using Deep VentR DNA Polymerase (New England Biolabs, Beverley, MA).

SF9 cell infection and whole cell extract preparation was performed as described by O'Reilly (36).

cDNA sequences of human and mouse *NUFIP* genes

Mouse sequence was derived from a 1657 bp cDNA sequence ended by a poly(A) tail established from two hybrid selected

clones in yeast. Three clones of the same size were selected from a mouse fetal brain cDNA library and the EST clones AA185054, AA219909 and AA139817. The human sequence (3462 bp) was established from the two EST clones AA397665 and AA214642 [with a poly(A) tail].

Construction of *mNUFIP* vectors

The original pASV3 (33) plasmid was digested with *Sfi*I and the insert subcloned in the *Sfi*I site of a modified pBluescript vector. Then this construct was digested with *Xho*I and *Sac*I and the insert cloned in pTL1 vector, producing pTL-mNUFIP. The insert from pTL-mNUFIP was subcloned into the pEGFP-C2 vector for expression of the GFP-fusion, producing GFP–mNUFIP.

Construction of *hNUFIP* vectors

The two overlapping EST clones AA397665 and AA214642 were digested with *Eco*RI–*Pst*I and *Pst*I–*Kpn*I, respectively, and cloned in the *Eco*RI and *Kpn*I sites of the vector pTL1. This plasmid was named pTL-hNUFIP. The plasmid pTL-hNUFIP was digested with *Eco*RI and cloned in the pEGFP-C2 vector (Clontech, Palo Alto, CA), producing GFP–hNUFIP. Deletion constructs were constructed by amplification of the plasmid pTL-hNUFIP with the forward primers GGGGAATTCATGCCTGCAGTTAAAAATTC, GGGGAATTCATGTTTAAAAATCAAGAAAAG and GGGGAATTCATGGAAAGGAAGAAGAAGTTAAAAC, all containing an *Eco*RI site, and the reverse primer GGGGTACCCTATACATCTTTACTTTTCGC, containing a *Kpn*I site. The fragments, digested with *Eco*RI and *Kpn*I, were cloned in pTL1 vector. PCR was performed as described above.

Antibody against hNUFIP

A synthetic polypeptide ENRKKSFEKTNPKRKKDYHN corresponding to amino acids 421–442 of the hNUFIP was coupled to ovalbumin (Ovalbumin-MBS; Sigma-Aldrich) and used for immunization of rabbits using standard protocols. The antiserum was purified on an affinity column coupled to the same peptide used for immunization, according to the manufacturer's instructions (Sulfolink coupling gel; Pierce, Rockford, IL).

GST pull-down assay

Full-length and deletion constructs were produced by *in vitro* transcription-translation in rabbit reticulocyte lysate or wheat germ extract in the presence of [^{35}S]methionine (ICN, Orsay, France), according to the manufacturer's instructions (Promega, Madison, WI).

In vitro translated proteins were mixed with 1 mg of GST-fused protein (FMRP produced in a baculovirus system or hNUFIP produced in bacteria) or with 1 mg of GST. GST pull-down assays were carried out in the following buffer: 20 mM Tris–HCl pH 7.5, 100/200/500 mM NaCl, 5 mM EGTA, 1% Triton X-100, 1 mM phenylmethylsulfonyl fluoride (PMSF), as described (24).

Immunoprecipitation

HeLa cells or transfected COS cells were lysed in the following buffer: 500 mM NaCl, 20 mM Tris–HCl pH 7.5, 2% Triton X-100, 1 mM PMSF. The immunoprecipitation was carried out in the lysis buffer as described (37) and indicated in the legends to the figures. The proteins bound to the beads were separated by electrophoresis on 8–12% SDS–polyacrylamide gel and visualized by immunoblot using the 1C3 antibody (8), no. 566 antibody (28) or no. 1375 (this study).

Construction of human *FXR1* and *FXR2* vectors

FXR1 and *FXR2* (30) were amplified using the forward primers GGGAATTCATGGCGGACGTGACGGTGGAGG and GGGAATTCATGGGCGGCCTGGCCTCTGG, both containing an *Eco*RI restriction site, and the reverse primers GGGCGATCGCCATGCAAGTTGTTTTGTGCATTCTAAATGC, containing a *Pst*I restriction site, and GGGAGATCTGGCTGCTGCCAACTGCTTGCTTG, containing a *Bgl*II restriction site. The PCR fragments were digested with *Eco*RI and *Pst*I or *Eco*RI and *Bgl*II, respectively, cloned in the vector pBTM116m (27), and digested with the appropriate restriction enzymes. The PCR reaction was as described above. Yeast strain L40 was transformed with pASV3-mNUFIP and pBTM-FXR1 or pBTM-FXR2; β-galactosidase activity was evaluated as described (27).

Cell transfection and immunofluorescence detection

Transfection of COS and HeLa cells, cell fixation and immunodetection with the 1C3 monoclonal antibody were carried out as previously described (11). Polyclonal antibody no. 1375 was diluted 1:8000. Double-label immunofluorescence experiments were performed by separate sequential incubations of each primary antibody diluted in phosphate-buffered saline (PBS) (incubation at 4°C overnight), followed by the specific secondary coupling to TXRD or OG (Jackson Immunoresearch Laboratories, West Grove, PA) (incubation at room temperature for 1 h). The light microscope was a Leica (Wetzlar, Germany) LEITZ DMRD. Confocal images were obtained with a Leica TCS4D microscope. Images were colourized and merged using the Adobe Photoshop software program.

In situ hybridization on tissue sections

In order to obtain sense and antisense RNA probes, *mNUFIP* and *FMR1* cDNAs cloned in pBluescript were linearized by digestion with *Xho*I or *Sac*I and with *Eco*RI or *Spe*I, respectively. *In vitro* transcription and *in situ* hybridization were performed as previously described (38).

Production and purification of NUFIP recombinant protein in bacteria

The *hNUFIP* gene was cloned in the *Eco*RI site of the pGEX-4T1 (Pharmacia, Uppsala, Sweden) expression vector and transformed in the BL21 bacterial strain. After induction with 0.5 mM isopropyl-b-D-thiogalactopyranoside (IPTG) for 24 h at 25°C, purification of the protein was performed according to the manufacturer's instructions (Pharmacia).

RNA-binding assays

Ribonucleotide homopolymer-binding assays were carried out as previously described (13,29). Preparation of the probes and north-western blot analysis were carried out as previously described (39).

ACKNOWLEDGEMENTS

We are indebted to E. Lalli, A. Lunkes, D. Bartholdi and Y. Shen for suggestions and gifts of materials. We thank G. Duval, P. Eberling, I. Kolb-Cheynel, A. L'Honoré, N. Messadeqq, S. Pannetier, R. Redon, S. Vicaire, J.L. Vonesch, J.L. Weickert, the culture service and the graphic service of IGBMC for help in this work. This study was supported by funds from the Institut National de la Santé et de la Recherche Médicale, the Centre National de la Recherche Scientifique, and the Hôpital Universitaire de Strasbourg. B.B. is an investigator of the Dipartimento Patologia Umana ed Ereditaria dell'Universitá di Pavia (Italy) and was supported by the Italian Telethon and Fondation pour la Recherche Médicale.

REFERENCES

1. Hagerman, R.J. (1992) In Hagerman, R.J and Silverman, A.C. (eds), *Fragile X Syndrome: Diagnosis, Treatment and Research*. Johns Hopkins University Press, Baltimore, MD, pp. 1–68.
2. Oberlé, I., Rousseau, F., Heitz, D., Kretz, C., Devys, D., Hanauer, A., Boue, J., Bertheas, M.F. and Mandel, J.L. (1991) Instability of a 550-base pair DNA segment and abnormal methylation in fragile X syndrome. *Science*, **252**, 1097–1102.
3. Verkerk, A.J.M.H., Pieretti, M., Sutcliffe, J.S., Fu, Y.H., Kuhl, D.P.A., Pizzuti, A., Reiner, O., Richards, S., Victoria, M.F., Zhang, F., Eussen, B.E., Van Ommen, G.J.B., Blonden, L.A.J., Riggins, G.J., Chastain, J.L., Kunst, C.B., Galjaard, H., Caskey, C.T., Nelson, D.L., Oostra, B.A. and Warren, S.T. (1991) Identification of a gene (FMR-1) containing a CGG repeat coincident with a breakpoint cluster region exhibiting length variation in fragile X syndrome. *Cell*, **65**, 905–914.
4. Kremer, E.J., Pritchard, M., Lynch, M., Yu, S., Holman, K., Baker, E., Warren, S.T., Schlessinger, D., Sutherland, G.R. and Richards, R.I. (1991) Mapping of DNA instability at the Fragile X to a trinucleotide repeat sequence $(pCCG)_n$. *Science*, **252**, 1711–1714.
5. Sutcliffe, J.S., Nelson, D.L., Zhang, F., Pieretti, M., Caskey, C.T., Saxe, D. and Warren, S.T. (1992) DNA methylation represses FMR-1 transcription in fragile X syndrome. *Hum. Mol. Genet.*, **1**, 397–400.
6. Verkerk, A.J., de Graaff, E., De Boulle, K., Eichler, E.E., Konecki, D.S., Reyniers, E., Manca, A., Poustka, A., Willems, P.J., Nelson, D.L. and Oostra, B.A. (1993) Alternative splicing in the fragile X gene *FMR1*. *Hum. Mol. Genet.*, **2**, 399–404.
7. Eichler, E.E., Richards, S., Gibbs, R.A. and Nelson, D.L. (1993) Fine structure of the human *FMR1* gene. *Hum. Mol. Genet.*, **2**, 1147–1153.
8. Devys, D., Lutz, Y., Rouyer, N., Bellocq, J.P. and Mandel, J.L. (1993) The FMR-1 protein is cytoplasmic, most abundant in neurons and appears normal in carriers of a fragile X premutation. *Nature Genet.*, **4**, 335–340.
9. Wohrle, D., Fryns, J.P. and Steinbach, P. (1990) Fragile X expression and X inactivation. I. The expression of the fragile site at Xq27.3 is not suppressed on inactive X chromosomes separated from the active homologue. *Hum. Genet.*, **85**, 659–665.
10. Verheij, C., de Graaff, E., Bakker, C.E., Willemsen, R., Willems, P.J., Meijer, N., Galjaard, H., Reuser, A.J.J., Oostra, B.A. and Hoogeveen, A.T. (1995) Characterization of FMR1 proteins isolated from different tissues. *Hum. Mol. Genet.*, **4**, 895–901.
11. Sittler, A., Devys, D., Weber, C. and Mandel, J.L. (1996) Alternative splicing of exon 14 determines nuclear or cytoplasmic localisation of fmr1 protein isoforms. *Hum. Mol. Genet.*, **5**, 95–102.
12. Siomi, H., Siomi, M.C., Nussbaum, R.L. and Dreyfuss, G. (1993) The protein product of the fragile X gene, FMR1, has characteristics of an RNA-binding protein. *Cell*, **74**, 291–298.
13. Siomi, H., Choi, M., Siomi, M.C., Nussbaum, R.L. and Dreyfuss, G. (1994) Essential role for KH domains in RNA binding: impaired RNA binding by a mutation in the KH domain of FMR1 that causes fragile X syndrome. *Cell*, **77**, 33–39.
14. Ashley, C.T., Sutcliffe, J.S., Kunst, C.B., Leiner, H.A., Eichler, E.E., Nelson, D.L. and Warren, S.T. (1993) Human and murine FMR-1: alternative splicing and translational initiation downstream of the CGG-repeat. *Nature Genet.*, **4**, 244–251.
15. Corbin, F., Bouillon, M., Fortin, A., Morin, S., Rousseau, F. and Khandjian, E.W. (1997) The fragile X mental retardation protein is associated with poly(A)$^+$ mRNA in actively translating polyribosomes. *Hum. Mol. Genet.*, **6**, 1465–1472.
16. Feng, Y., Absher, D., Eberhart, D.E., Brown, V., Malter, H.E. and Warren, S.T. (1997) FMRP associates with polyribosomes as an mRNP and the I304N mutation of severe fragile X syndrome abolishes this association. *Mol. Cell*, **1**, 109–118.
17. Eberhart, D.E., Malter, H.E., Feng, Y. and Warren, S.T. (1996) The Fragile X mental retardation protein is a ribonucleoprotein containing both nuclear localization and nuclear export signals. *Hum. Mol. Genet.*, **5**, 1083–1091.
18. Bardoni, B., Sittler, A., Shen, Y. and Mandel, J.L. (1997) Analysis of domains affecting intracellular localization of the FMRP protein. *Neurobiol. Dis.*, **4**, 329–336.
19. Fridell, R.A., Benson, R.E., Hua, J., Bogerd, H.P. and Cullen, B.R. (1996) A nuclear role for the Fragile X mental retardation protein. *EMBO J.*, **15**, 5408–5414.
20. Tamanini, F., Bontekoe, C., Bakker, C.E., van Unen, L., Anar, B., Willemsen, R., Yoshida, M., Galjaard, H., Oostra, B.A. and Hoogeveen, A.T. (1999) Different targets for the fragile X-related proteins revealed by their distinct nuclear localizations. *Hum. Mol. Genet.*, **8**, 863–869.
21. Imbert, G., Feng, Y., Nelso, D.L., Warren, S.T and Mandel, J.L. (1998) In Warren, S.T and Hayden, M.R. (eds), *Genetics Instabilities and Hereditary Neurological Diseases*. Academic Press, San Diego, CA, pp. 27–53.
22. Siomi, M.C., Siomi, H., Sauer, W.H., Srinivasan, S., Nussbaum, R.L. and Dreyfuss, G. (1995) FXR1, an autosomal homolog of the fragile X mental retardation gene. *EMBO J.*, **14**, 2401–2408.
23. Zhang, Y., O'Connor, J.P., Siomi, M.C., Srinivasan, S., Dutra, A., Nussbaum, R.L. and Dreyfuss, R. (1995) The fragile X mental retardation syndrome protein interacts with novel homologs FXR1 and FXR2. *EMBO J.*, **14**, 5358–5366.
24. Siomi, M.C., Zhang, Y., Siomi, H. and Dreyfuss, G. (1996) Specific sequences in the fragile X syndrome protein FMR1 and FXR proteins mediate their binding to 60S ribosomal subunits and the interactions among them. *Mol. Cell. Biol.*, **16**, 3825–3832.
25. Tamanini, F., Willemsen, R., van Unen, L., Bontekoe, C., Galjaard, H., Oostra, B.A. and Hoogeveen, A.T. (1997) Differential expression of FMR1, FXR1 and FXR2 proteins in human brain and testis. *Hum. Mol. Genet.*, **6**, 1315–1322.
26. Fields, S. and Song, O. (1990) A novel genetic system to detect protein interactions. *Nature*, **340**, 245–246.
27. Vojtek, A.B., Hollenberg, S.M. and Cooper, J.A. (1993) Mammalian Ras interacts directly with the serine/threonine kinase Raf. *Cell*, **74**, 205–214.
28. Lunkes, A. and Mandel, J.L. (1998) A cellular model that recapitulates major pathogenic steps of Huntington's disease. *Hum. Mol. Genet.*, **7**, 1355–1361.
29. Brown, V., Small, K., Lakkis, L., Feng, Y., Gunter, C., Wilkinson, K.D. and Warren, S.T. (1998) Purified recombinant FMRP exhibits selective RNA binding as an intrinsic property of the fragile X mental retardation protein. *J. Biol. Chem.*, **273**, 15521–15527.
30. Khandjian, E.W., Bardoni, B., Corbin, F., Sittler, A., Giroux, S., Heitz, D., Tremblay, S., Pinset, C., Montarras, D., Rousseau, F. and Mandel, J.L. (1998) Novel isoforms of the fragile X related protein FXR1P are expressed during myogenesis. *Hum. Mol. Genet.*, **7**, 2121–2128.
31. La Morte, V.J., Dyck, J.A., Ochs, R.L. and Evans, R.M. (1998) Localization of nascent RNA and CREB binding protein with the PML-containing nuclear body. *Proc. Natl Acad. Sci. USA*, **95**, 4991–4996.
32. Gietz, D., St Jean, A., Woods, R.A. and Schiestl, R.H. (1992) Improved method for high efficiency transformation of intact yeast cells. *Nucleic Acids Res.*, **20**, 1425.
33. Le Douarin, B., Pierrat, B., vom Baur, E., Chambon, P. and Losson, R. (1995) A new version of the two-hybrid assay for detection of protein–protein interactions. *Nucleic Acids Res.*, **23**, 876–878.

34. Ausubel, F.M., Brent, R., Kingston, R.E., Moore, D.D., Seidman, J.G., Smith, J.H and Stuhl, K. (1987) *Current Protocols in Molecular Biology*. Greene Publishing Associates and Wiley Interscience, New York, NY, pp. 13.6.2–13.6.24.
35. Acker, J., de Graaff, M., Cheynel, I., Khazak, V., Kedinger, C. and Vigneron, M. (1997) Interactions between the human RNA polymerase II subunits. *J. Biol. Chem.*, **272**, 16815–16821.
36. O'Reilly, D.R. (1997) Use of baculovirus expression vectors. *Methods Mol. Biol.*, **62**, 235–246.
37. Bertolotti, A., Lutz, Y., Heard, D.J., Chambon, P. and Tora, L. (1996) hTAF(II)68, a novel RNA/ssDNA-binding protein with homology to the pro-oncoproteins TLS/FUS and EWS is associated with both TFIID and RNA polymerase II. *EMBO J.*, **15**, 5022–5031.
38. Schaeren-Wiemers, N. and Gerfin-Moser, A. (1993) A single protocol to detect transcripts of various types and expression levels in neural tissue and cultured cells: *in situ* hybridization using digoxigenin-labelled cRNA probes. *Histochemistry*, **100**, 431–440.
39. Bertrandy, S., Burlet, P., Clermont, O., Huber, C., Fondrat, C., Thierry-Mieg, D., Munnich, A. and Lefevre, S. (1999) The RNA-binding properties of SMN: deletion analysis of the zebrafish orthologue defines domains conserved in evolution. *Hum. Mol. Genet.*, **8**, 775–782.